Substructuring of a nonlinear beam using a modal Iwan framework, Part I: Nonlinear Modal Model Identification

Daniel Roettgen,
Matthew S. Allen,
Daniel Kammer
Department of Engineering Physics
University of Wisconsin
Madison, WI 53706
droettgen@wisc.edu, msallen@engr.wisc.edu, kammer@engr.wisc.edu
Randy Mayes
Sandia National Laboratories
Albuquerque, NM
rlmayes@sandia.gov

Abstract:

This work uses a method whereby weak nonlinearity in a substructure, as typically arises due to microslip in bolted interfaces, can be captured and modeled on a mode-by-mode basis. The method relies on the fact that the modes of a weakly nonlinear structure tend to remain uncoupled so long as their natural frequencies are distinct and higher harmonics generated by the nonlinearity do not produce significant response in other modes. A single degree-of-freedom (DOF) system with an Iwan joint, which is known as a modal Iwan model, effectively captures the way in which the stiffness and damping depend on amplitude for each mode. This work presents the experiments used to generate these modal Iwan models. In a companion paper this model is assembled to another component using dynamic substructuring techniques to estimate the amplitude dependent frequency and damping of the full assembly.

Keywords: Experimental Nonlinear Detection, Nonlinear Modeling, Modal Iwan Models

Sandia National Laboratories is a multi-program laboratory managed and operated by Sandia Corporation, a wholly owned subsidiary of Lockheed Martin Corporation, for the U.S. Department of Energy's National Nuclear Security Administration under contract DE-AC04-94AL85000.

1. Introduction

Experimental-analytical substructuring allows one to predict the dynamic response of an assembly by coupling substructures derived from experiments with substructures represented by finite element models. There are numerous applications of experimental-analytical substructuring, but in particular this is useful when one has a subcomponent of a system that is difficult to model. When using subcomponents to predict the response of an assembly there are often many joints in the structure; either contained within a given subcomponent or in between two of them. Such joints are known to be a significant source of nonlinear damping in built up assemblies. Capturing these nonlinear joint dynamics in an experimental subcomponent model is one way to account for these dynamics when predicating responses for the full assembly. This work outlines methods used for testing structures with weakly nonlinear joints by using a recently proposed framework that models the structure as a collection of uncoupled, weakly nonlinear (in the case of micro-slip) oscillators. These nonlinear modal-like models are used in a companion paper, " Substructuring of a nonlinear beam using modal Iwan framework, Part II: Nonlinear Modal Substructuring" [1] in order to complete substructuring predictions. This paper addresses the detection, identification, and verification of these models on subcomponent structures.

The nonlinear models in this paper build on the efforts of Segalman, and his colleagues at Sandia National Laboratories, who pursued a multi-year project in which models for mechanical joints were derived and calibrated to match experimental force-dissipation measurements [2, 3]. They showed that one can determine the parameters for each joint in a structure and employ nonlinear time integration to compute the response including the effects of the joints. More recently, Segalman proposed to model each mode of a structure as independent but with an Iwan joint in parallel with the modal stiffness to capture the nonlinear damping (and to a lesser extent nonlinear stiffness) of the joint [4]. Using this method one can identify amplitude dependant modal stiffness and damping for each mode. Allen and Deaner extended Segalman's work by adding a viscous damper in parallel with the Iwan element to account for the linear material damping that dominates for each mode at

very small amplitudes [5] and began to more thoroughly explore the extent to which this modal approximation is accurate for real structures with several joints [6]. The approach used here is similar to that which was first used by Deaner to characterize a beam with a bolted joint. However, this work presents an updated means of interpreting the dissipation in the modal Iwan model that allows one to more clearly see how the damping ratio changes with response amplitude [7], while still allowing power-law behavior to be identified. In industry, modeling nonlinearities is often avoided by testing the structure at single amplitude, with the expectation that the resulting linearized model will be relevant in the environment of interest or the worst case environment. However, even though the idea is generally sound, when nonlinearities are ignored it is likely that the resulting model will be inaccurate because each mode may activate the nonlinearity at a different amplitude.

The paper is organized as follows. Section 2 outlines the theory behind the toolbox used for detection and identification of nonlinear modal models. Section 3 contains details about the test specimen, the Brake-Reuss Beam (BRB), and experimental set-up information. In Section 4 these techniques are validated by generating nonlinear modal models for the Brake-Reuss Beam system using modal Iwan models. A simulation of these models is then compared to that of the true structure. Section 5 concludes the paper and discusses some future work in this research area. This work continues in Part II [1] where these modal models are used in a dynamic substructuring prediction.

2. Nonlinear Modal Models

This section contains an overview of our latest process for experimental detection and characterization of nonlinear modal behavior. Figure 1 shows the steps of the processes we go through to detect, characterize and verify these nonlinear modal models. The goal is to highlight each step of the process and give insight into the different tools used when looking for nonlinear modal behavior in an experimental system. A more rigorous explanation to many of these tools is contained in [7].

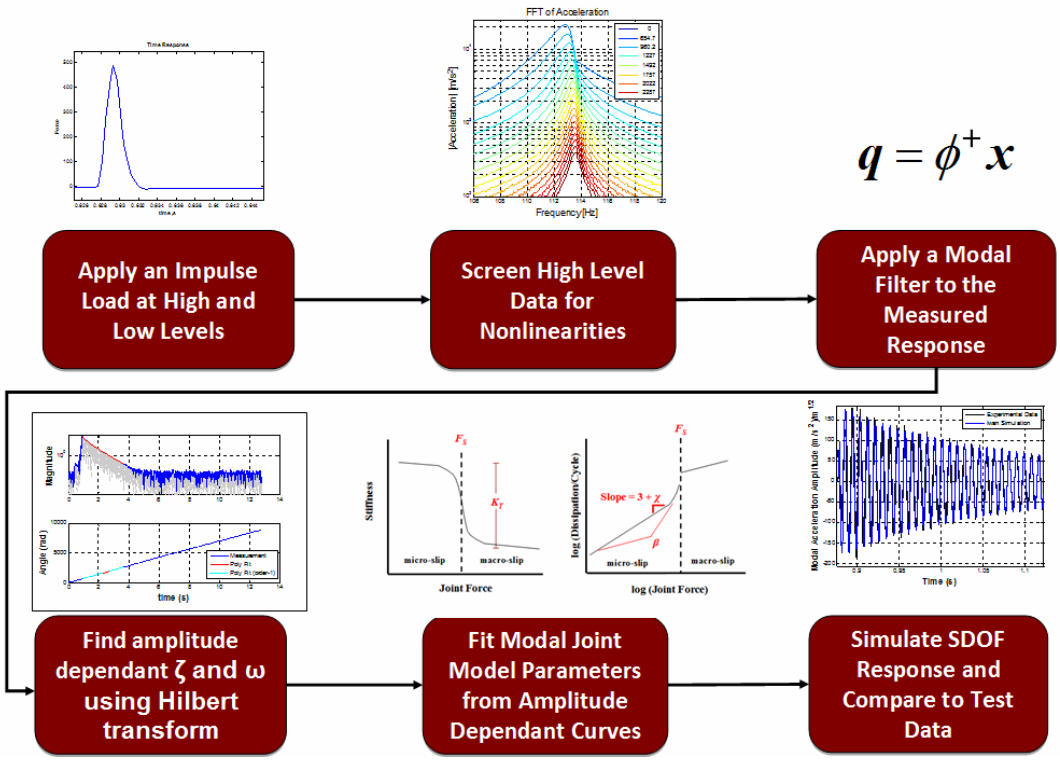

Figure 1. Nonlinear Modal Behavior Workflow

The fundamental equation or motion for a structure can be written as:

$$\mathbf{M}\ddot{x} + \mathbf{C}\dot{x} + \mathbf{K}x + F_j(x,\theta) = F \tag{1}$$

where $\mathbf{M}$, $\mathbf{C}$, and $\mathbf{K}$ represent the linear mass, damping and stiffness matrices, F is the excitation force and F_j is a nonlinear force due to the joints in the structure. Each mode is assumed to be independent and its mode shape is assumed to

remain the same as in the low-level linear system. These assumptions remain valid as long as the jointed structure remains weakly nonlinear and the modes remain uncoupled and are not closely spaced. [7, 8]

To begin identifying the nonlinear modal models contained in F_j, the structure is excited with an impulsive load at high and low force levels. The low force level measurement is used to find linear modal parameters as is the common practice in industrial applications. Next, the high load level data is used to screen each mode for nonlinear behavior.

Often in weakly nonlinear structures very small frequency shifts are observed but, large changes in damping are seen as amplitude increases. These differences are apparent when once compares the modal parameters extracted from a high forcing level impact test with those from a low forcing level. Additionally, comparing the frequency response function of the measured signals can provide insight as to how the response of the system changes at high and low amplitudes. All measurements are related to one modal response, thus the following equation can be solved in a least squares sense to obtain the modal amplitude from the acceleration measurements,

$$\boldsymbol{\varphi}_r \ddot{q}_r(t) = \ddot{x}(t) \tag{2}$$

where $\boldsymbol{\varphi}_r$ is the rth mass-normalized mode vector, $\ddot{q}_r(t)$ is the corresponding modal response and $\ddot{x}(t)$ is a vector of accelerations that were measured during a single-impact hammer test. This method allows multiple hammer strikes to be compared even from different driving point locations.

Each mode can now be represented as a single degree-of-freedom (SDOF) system as shown in Fig. 2. This SDOF system contains a modal mass which is tied to ground with a linear spring and damper. Also, a nonlinear element representing the joint force is also connected to this mass which can be used to describe the nonlinear behavior of this modal response. This nonlinear element could take many forms but for this work a 4-parameter Iwan element is used to represent this nonlinear joint force.

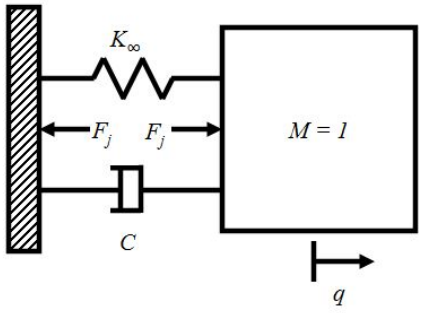

Figure 2. Schematic of SDOF model used for each modal degree of freedom

The original equation of motion can now be written in modal coordinates as shown in Eqn. (3).

$$\mathbf{I}\ddot{q} + \left[\backslash \left(2\zeta_0 \omega_0 \right)_\backslash \right] \dot{q} + \left[\backslash \left(\omega_0^{\,2} \right)_\backslash \right] q + \left\{ F_j \right\} = \boldsymbol{\phi}^T F \tag{3}$$

The next step in the process is to quantify the change in frequency and damping with amplitude. This is accomplished using the Hilbert transform algorithm as detailed in [5, 9]. This approach fits the modal response, $q(t)$, to the following analytic functional form:

$$\ddot{q}(t) = e^{\psi_r(t) + i\psi_i(t)} \tag{4}$$

where $\psi_r(t)$ and $\psi_i(t)$ are a series of splines in time and are, respectively, the real and imaginary parts of the time varying response model. The damped natural frequency can be related to the phase of the analytic signal as was discussed in [5]. Obtaining the damping ratio is covered in detail [7] but relates to both the amplitude and phase of the analytic signal. Based on the derivations mentioned the modal parameters can be obtained as shown in Eqn. (5). In addition to describing the nonlinear characteristics of the mode, these parameters also allow for the conversion of modal acceleration to modal velocity and displacement.

$$\omega_d(t) \triangleq \frac{d\psi_i}{dt} \qquad -\zeta\omega_n(t) \triangleq \frac{d\psi_r}{dt} \tag{5}$$

Recall, each mode will be modeled with a single degree of freedom system with a spring, damper, and nonlinear joint force which is modeled as a 4-Parameter Iwan model. This joint force can be written in the following form,

$$F_j(t) = \int_0^\infty \rho(\phi)\left[u(t) - x(t,\phi)\right] d\phi \tag{6}$$

where F_j is the force in the joint, u is joint displacement, ρ is a kernel that characterizes the joint and x is a continuum of state variables that evolve as

$$\dot{x}(t,\phi) = \begin{cases} \dot{u} \;\text{ if }\; \left\| u - x(t,\phi) \right\| \\ \qquad \text{and } \; \dot{u}\left(u - x(t,\phi)\right) > 0 \\ 0 \quad \text{otherwise} \end{cases} \tag{7}$$

The form of the kernel, $\rho(\phi)$, is discussed in detail in [3] and can be defined by four parameters, $[F_s,\ K_T,\ \chi,\ \beta]$, where F_s is the joint force required to begin macro-slip, K_T is the stiffness in the joint, χ is related to the exponent in the power-law relationship between damping and amplitude in the micro-slip regime and β defines the shape of the dissipation curve near the transition from micro to macro-slip. This kernel was designed to reproduce the power-law damping that has been observed in experiments. When this joint model is used in a modal framework, these four parameters define the nonlinear characteristics of each mode in the system and can be obtained from experimental measurements as outlined in [5, 7].

3. Experimental System - Brake-Reuss Beam System

This process was applied to a bolted structure consisting of two half beams with a lap joint containing three individual bolts. This beam is known as the Brake-Reuss beam (BRB) system first researched by Brake and Reuss in [10]. The bolts in this assembly were tightened to the recommended 20 ft-lb torque [11]. This system has been studied by several groups at the Nonlinear Mechanics and Dynamics (NOMAD) institute hosted by Sandia National Labs in the past [12, 13]. The beam studied here consists of beam halves 1A and 1B from the 2015 NOMAD institute.

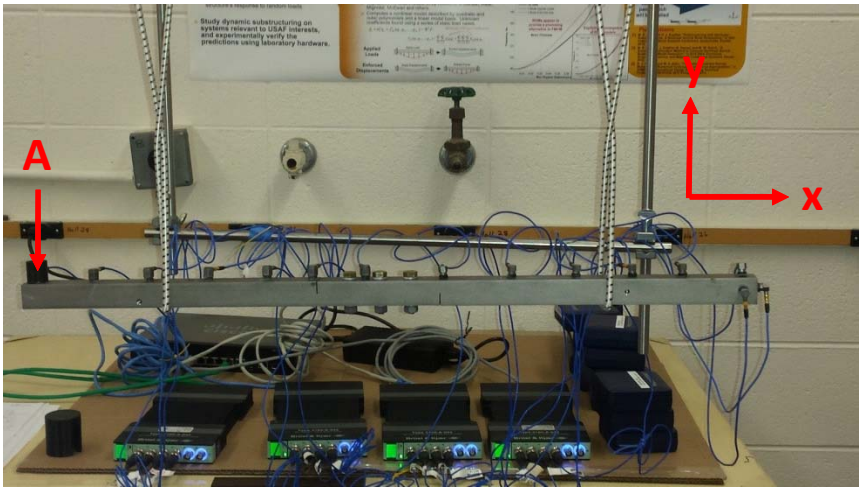

Figure 3. Photograph of Brake-Reuss beam system experimental set-up

The primary modes of interest in this study are the bending modes in the xy-plane as defined in Fig. 4. Based on previous experiments [12] the frequency range of interest was 0-2000 Hz, where the first few bending modes could be readily

obtained. The system was instrumented with 15 low sensitivity (5 mV/g) accelerometers, 13 of these sensors are in the primary direction of interest with 2 off-axis sensors for troubleshooting. Using low level hammer hits on the accelerometer at point A, the modal parameters of the first four bending modes were extracted from the test specimen. Figure 4 shows these bending modes for the measurement points in the y-direction.

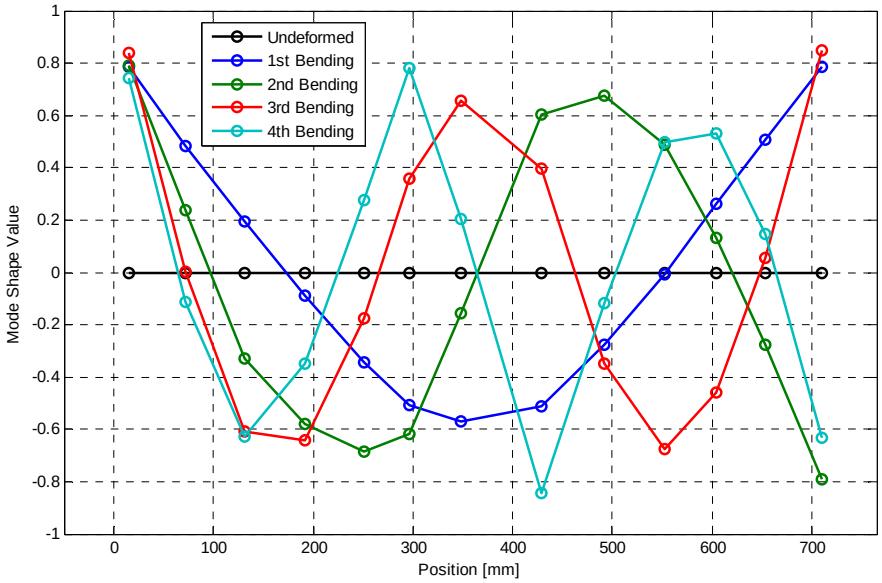

Figure 4. Bending mode shapes of Brake-Reuss beam structure

Table 1 contains a list of the natural frequencies and damping ratios extracted for each of the modes using the Algorithm of Mode Isolation (AMI), a linear modal parameter identification algorithm that is detailed in [14]. With linear modes defined, the next step is to screen these modes for nonlinear behavior and identify candidate nonlinear modal models.

Table 1: Linear (low amplitude) modal parameters

Elastic Mode Index	Natural Frequency [Hz]	Damping Ratio	Deflection Type
1	172.70	0.00095	1st Bending
2	583.26	0.00143	2nd Bending
3	1179.99	0.00376	3rd Bending
4	1645.43	0.00814	4th Bending

4. Nonlinear Modal Behavior: Detection and Model Identification

4.1 Nonlinear Model Behavior: Detection

With a linear model for the first four bending modes established, the structure was ready to be tested at higher impact levels in order to screen for nonlinearity. The assembly was probed by hitting the beam several times at varying load levels and at several drive points to deduce whether any modes might behave nonlinearly. By comparing the frequency response function for each of these hits we can see how the response of the first mode changes as force level is increased, see Figure 5. In a truly linear system all of these curves would overlay as the amplitude of the force and response would be linearly scaled. Due to the nonlinearities in the Brake-Reuss Beam assembly, increasing the impulsive force results in a slight decrease in the resonant frequency and an increase in the modal damping observed by the decreasing FRF amplitude. These changes are similar to what has been observed in the past when a nonlinear modal model was well suited to fit the response [7].

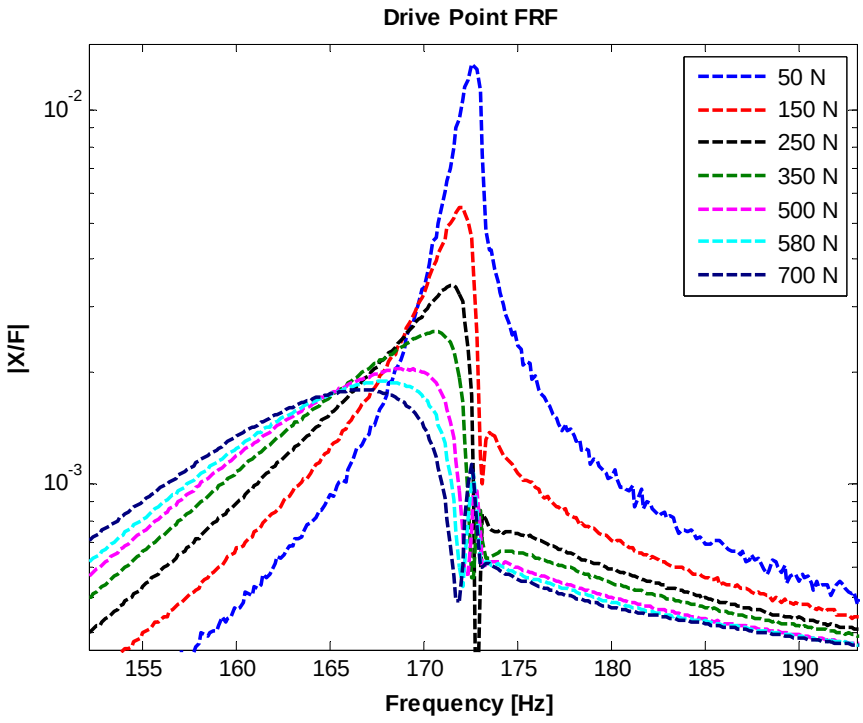

Figure 5. First bending mode multi-level frequency response function

While this frequency shift shows that the stiffness nonlinearity is quite small, this mode exhibited much more significant nonlinearity in damping. A similar analysis was performed on the second elastic mode, which also revealed a measurable shift in the natural frequency of over the same range of input force. The third and forth elastic modes showed smaller traces of nonlinearity so it was decided to create nonlinear modal models for the first two bending modes and use linear models for the third and fourth bending modes. A summary of the observed frequency and damping nonlinearities is shown in Table 2. The trends from this table are used solely to screen modes and make sure the results of the fit models are reasonable.

Table 2: Summary of results for Brake-Reuss Beam system NA = not applicable (linear mode)
** Damping Ratios obtained from Half Power Bandwidth of highest and lowest force level strikes*

Elastic Mode	Natural Frequency [Hz]	% Shift in Peak Frequency	Linear Damping Ratio*	Maximum Damping Ratio*	% Shift in Damping
1	172.70	-3.81%	0.00095	0.01060	+1015%
2	583.26	-1.28%	0.00143	0.00625	+337%
3	1179.99	NA	0.00376	NA	NA
4	1645.43	NA	0.00814	NA	NA

Now that the first two modes have been identified as nonlinear, their corresponding amplitude dependent stiffness and damping need to be obtained. A spatial filter is first applied to each of the measured data sets in order to isolate each mode as in Eqn. (2). This results in a SDOF response for each mode for each test run completed. The fast Fourier transform of these spatially filtered signals is shown in the Fig. 6. It is important to properly filter the signals into single harmonic, any contamination from closely spaced modes can cause major distortions when the stiffness and damping are fit versus amplitude.

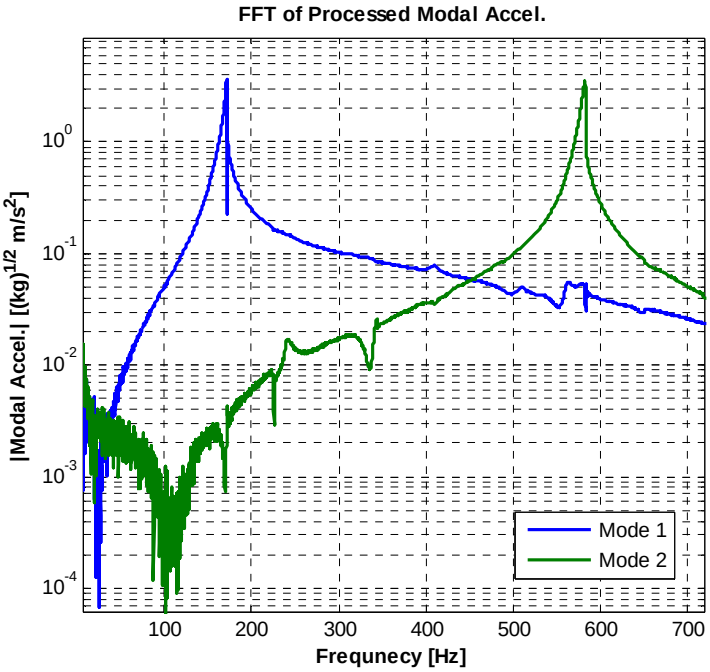

Figure 6. FFT of spatially filtered signals

Next, the Hilbert transform is used to obtain an expression in the form of Eqn. (4) for each single degree of freedom response. In order to achieve a higher quality fit of frequency and damping, a band-pass filter is applied to the modally filtered signal to ensure the signal is a single harmonic. Then a mirroring algorithm is used to mirror the time signal back in time directly after the impulse is applied. This mirroring makes the change in amplitude less abrupt and reduces the end effects in the Hilbert transform. Figure 7 shows this mirrored signal for the 1st bending mode. The magnified plots show that the signal has smoothly varying amplitude and hence will be well describe by the SDOF model.

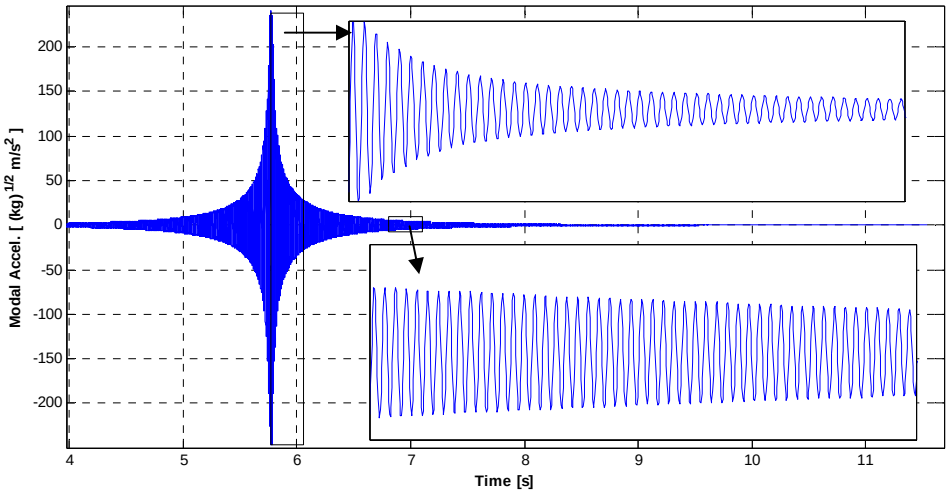

Figure 7. Mirrored signal of 1st bending mode modal acceleration

The envelope and phase of this mirrored signal was then fit to a spline with 30 knots as shown in Fig. 8. The top portion of the subplot shows a fit of the Hilbert envelope and the middle portion shows a fit of the unwrapped phase. Finally the bottom plot shows how well the Hilbert signal recreated the original spatially filtered response.

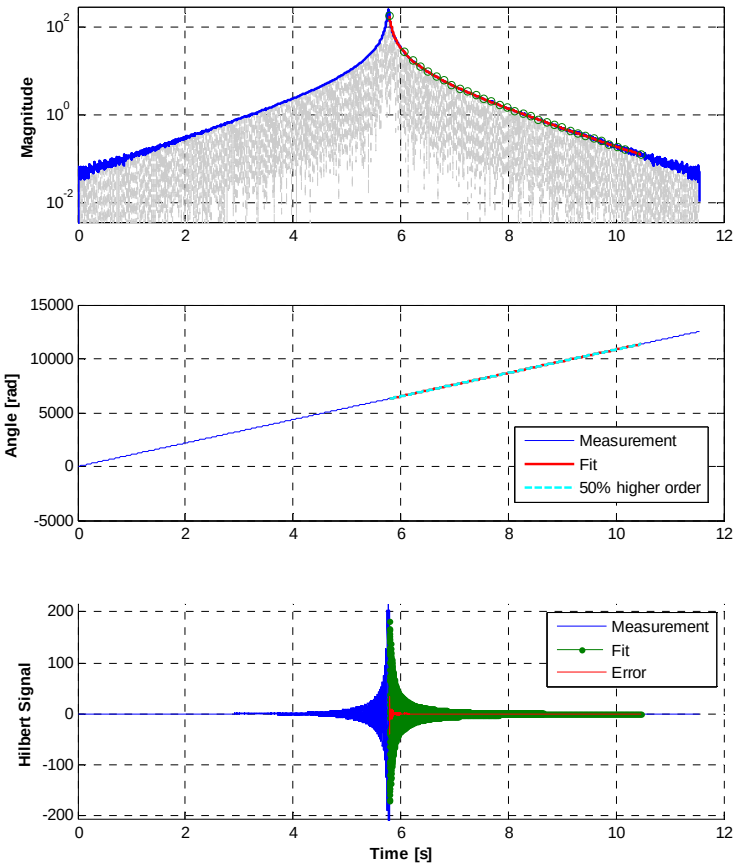

Figure 8. Hilbert fit for 1st bending mode: Hilbert Envelop (top), Hilbert Phase (middle),Reconstructed Signal (bottom)

Using the relationships from Eqn. (5), the fit envelope and phase can be related to the damping and stiffness of the signal. Plotting the damping and stiffness versus amplitude yields a relationship from which nonlinear modal model parameters can be extracted. Figure 9 and 10 show an example of this process for the 1st bending mode of the system where the damped natural frequency and damping ratio are plotted versus time and amplitude, respectively.

Note that later in time (lower in amplitude) a frequency is seen near 172.7 Hertz which is the linear frequency from modal testing in Table 1. Early in the time signal (when the modal amplitude is high) the frequency gets as low as 169 Hz, or about a 2% shift in frequency, close to what was observed by testing at multiple forcing levels as shown in Fig. 5. Similar comparisons can be seen in the linear damping ratio which matches the measurement present in Table 1. The nonlinear damping ratio reaches levels much higher than observed in the simple FRF screening process, most likely due to the half-power bandwidth assumption being used on a nonlinear data set.

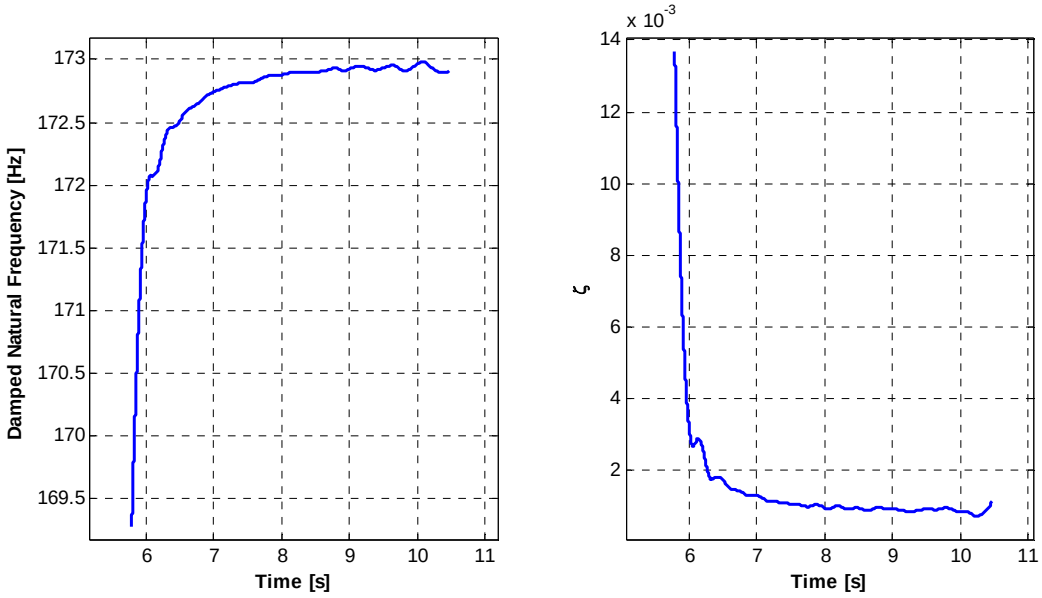

Figure 9. Hilbert fit for 1st bending stiffness and damping mode in time

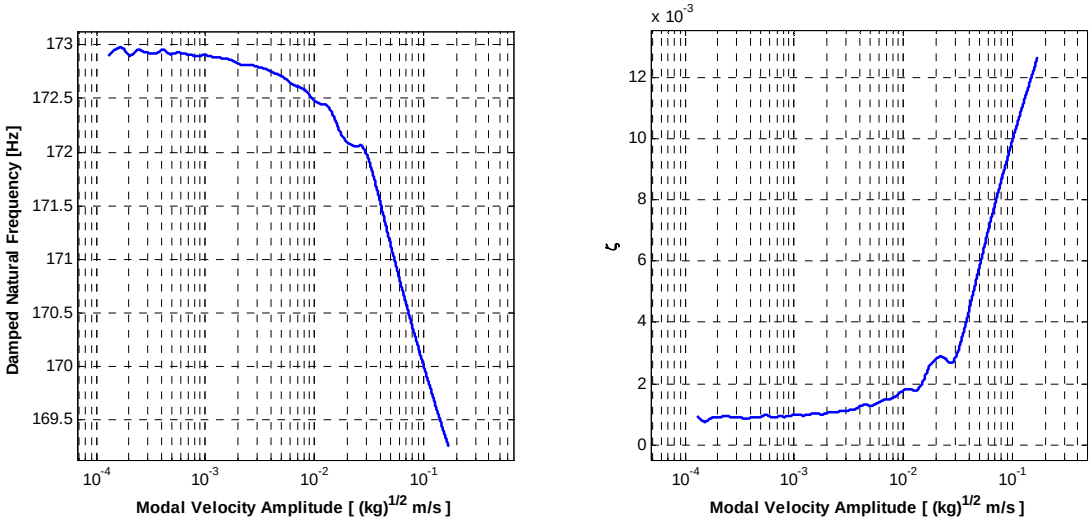

Figure 10. Amplitude dependant stiffness and damping curves

4.2 Nonlinear Model Behavior: Model Identification

The results shown in Figs. 9 and 10 were extracted from only one of the excitation amplitudes at which tests were performed. The spectra at various load levels are shown in Fig. 5. To ensure that the modes were adequately uncoupled, testing was also conducted from differing drive point locations. For each impact test a pair of stiffness and damping curves were generated. This ensemble of damped natural frequency and damping ratio curves for each nonlinear mode can be overlaid to see how repeatable these amplitude dependent measurements are. These overlaid curves were used to extract modal Iwan model parameters as shown in Fig. 11.

The modal Iwan model is defined by four parameters, $[F_s,\ K_T,\ \chi,\ \beta]$. To fit the dissipation parameter, χ, of the Iwan modal model these amplitude dependant damping curves were fit in a least squares sense. In this figure the total modal damping in the mode, extracted by the Hilbert transform, is given by the blue curves. Next, the linear contribution was removed from these curves revealing the nonlinear part of the damping in red (i.e. the part that is not linear and viscous). At low amplitudes this can be very noisy but at higher amplitudes a distinct trend is clear on this log-log scale. χ is then fit to this distinct high amplitude potion of the nonlinear damping curve by setting the slope of this curve equal to $\chi + 1$. This Iwan fit is shown in black. Finally to ensure the total modal damping is well simulated the linear portion of the damping is added back to the Iwan fit to obtain the total modal damping, shown in green.

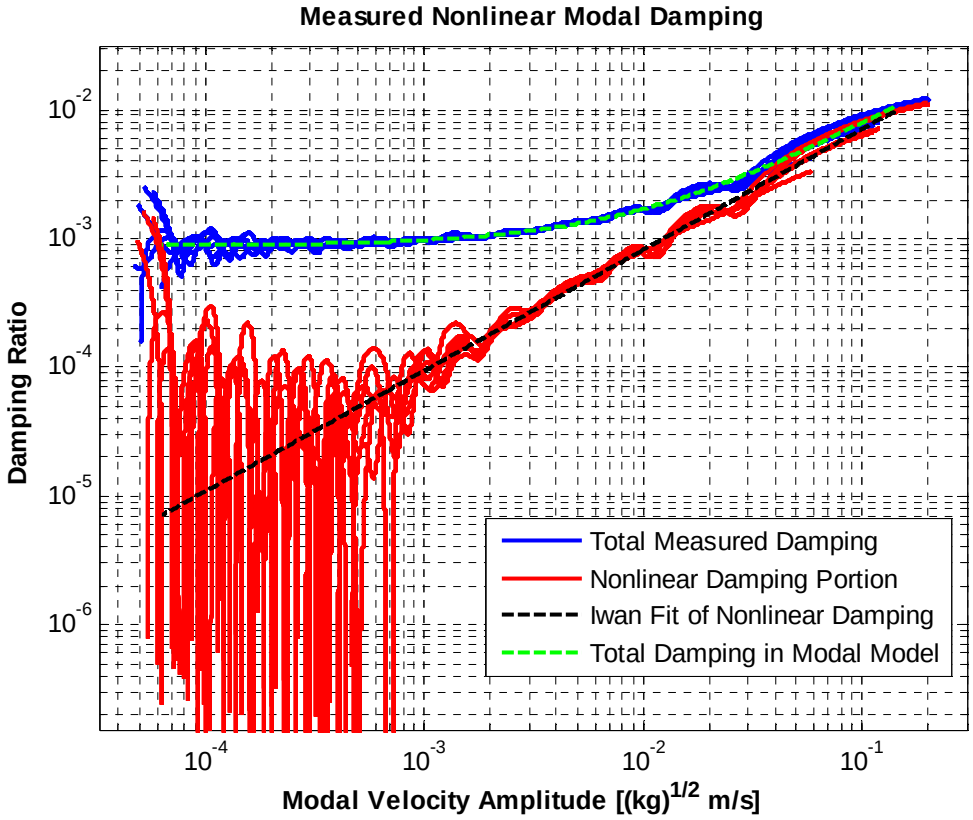

Figure 11. Measured Modal Damping for Mode 1

The other modal Iwan parameters are more ambiguous but were selected based off of engineering judgment and previous testing history. There was no obvious evidence of macro-slip in the experimental test; therefore, the slip force can be assumed to be greater than any of the excitations applied experimentally.

$$F_S \geq \varphi_{dp} F \tag{8}$$

The joint stiffness, K_T, is dependent on the frequency shift observed once the structure is in macro-slip, and because macro-slip wasn't achieved in these tests this parameter can't be readily estimated. This beam was previously tested by Bonney et. al. [12] and their tests included higher amplitude impacts where the macroslip frequency for the first mode was observed to be 130 Hz. This was used to estimate K_T using :

$$K_T = K_0 - K_\infty = \omega_0^2 - (\omega_0 - \omega_{shift})^2 \tag{9}$$

In principle, the parameter β can be found from the y-intercept of the dissipation versus amplitude curve, but in this case this would not be reliable since F_s and K_T are not known precisely. Instead β was assumed to be zero (corresponding to a case where the power law term in the Iwan model is much larger than the macro-slip term) and then varied to see whether the results were sensitive to that assumption.

These concepts were used to estimate starting values for the parameters and then they were varied until the frequency and damping versus amplitude curves of the modal Iwan model (found by integrating the SDOF equation of motion with the Newmark algorithm [15]) matched what was measured experimentally. Table 3 shows the final parameters that were used in order to model the first and second elastic modes.

Table 3: Iwan model parameters Brake-Reuss Beam System

Parameter	Simulation Case 1st Mode	Simulation Case 2nd Mode
F_s	137.72	152.14
K_T	484680	2668200
β	0.26159	0.29688
χ	-0.049947	-0.41637

The accuracy of these final parameters was initially checked by simulating a SDOF modal response to a singe impact for each nonlinear mode and comparing the results to the corresponding measured modal filtered signal. Figure 12 shows this comparison in the time domain for the first bending mode. Here, one can observe that in both early and late time the modal model closely matches the measured data.

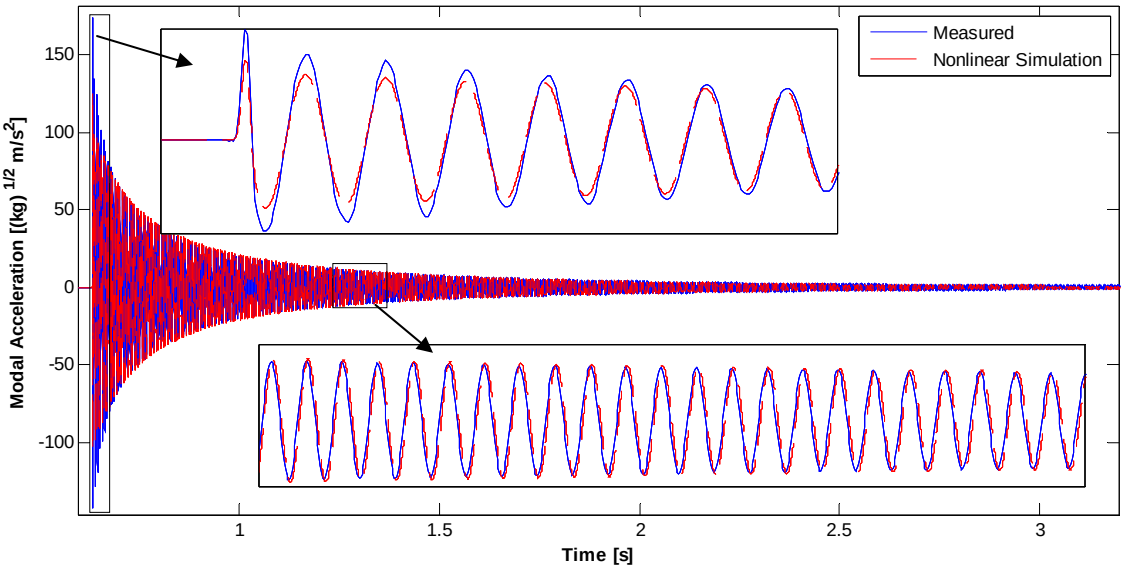

Figure 12. Modal Acceleration - 1st Elastic Mode

These responses can be further compared via their amplitude dependent stiffness and damping curves of each signal. These curves were extracted from the simulated response using the Hilbert transform as described previously. Figures 13 and 14 show the comparison between the measured and simulated response for the simulated loading case. The model obtains good correlation throughout the amplitude range of interest. A similar process was followed for the second bending mode leading to another nonlinear modal model. All of these figures show an excellent agreement between the model and measured data. Therefore the modal Iwan model with parameters from Table 3 sufficiently captures the nonlinear characteristics of the first two elastic modes.

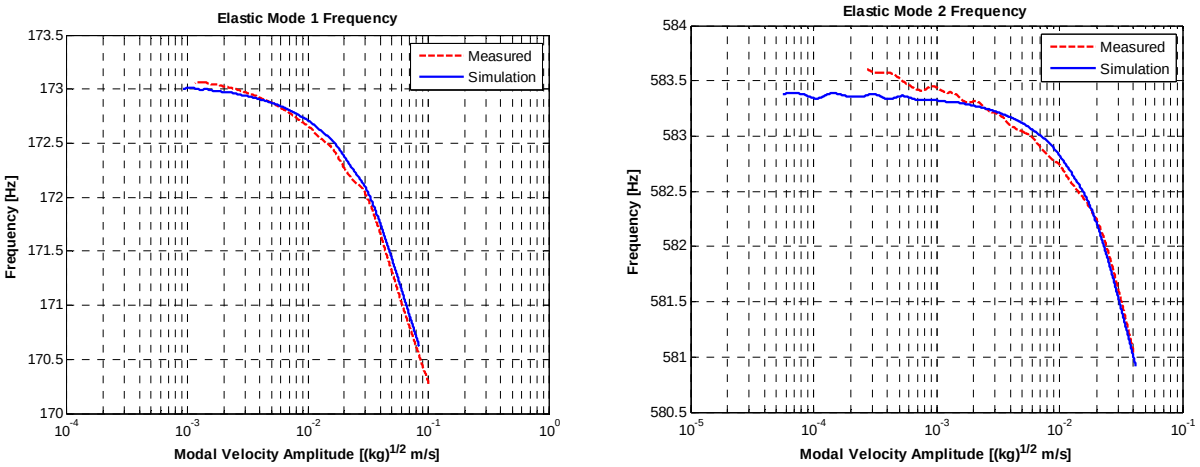

Figure 13. Measured and Simulated Modal Frequency for Elastic Modes 1 and 2

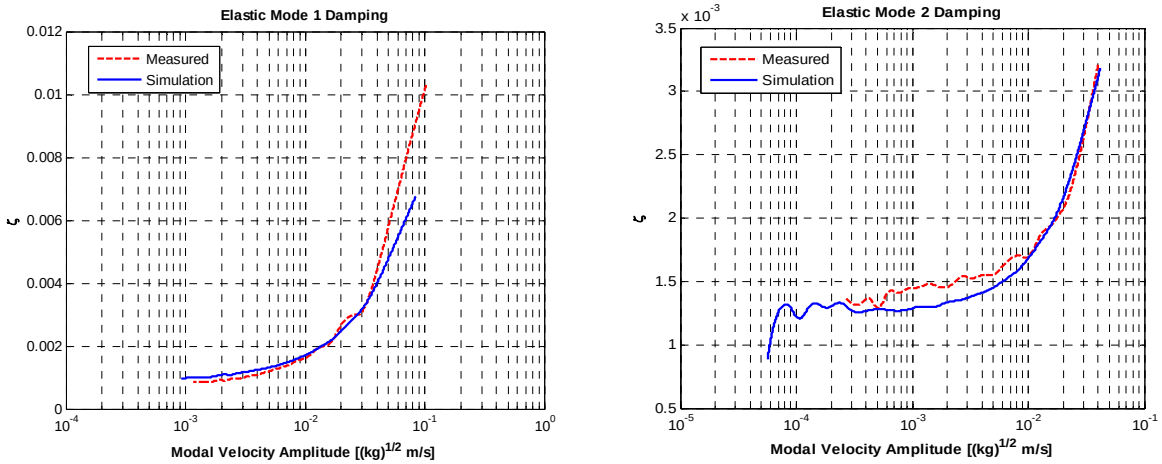

Figure 14. Measured and Simulated Modal Damping for Elastic Modes 1 and 2

With nonlinear modal models for the first two bending modes, the fidelity of the multi-modal model can now be assessed. The responses of four elastic modes were simulated due to modal forces corresponding to a 180 N impulsive force at drive point location A from Fig. 3. Each mode was integrated separately with the first two elastic modes using the nonlinear modal model in as in Eqn. (3). Once each single degree of freedom calculation was complete, the linear mode shape matrix was used to transform these results back into physical space. Figure 15 shows the simulated nonlinear and measured drive point acceleration responses. Note, a simulation was also conducted using a purely linear modal model using the parameters from Table 1. Here one can observe that the standard linear model over predicts the amplitude of response for a large majority of the ring down.

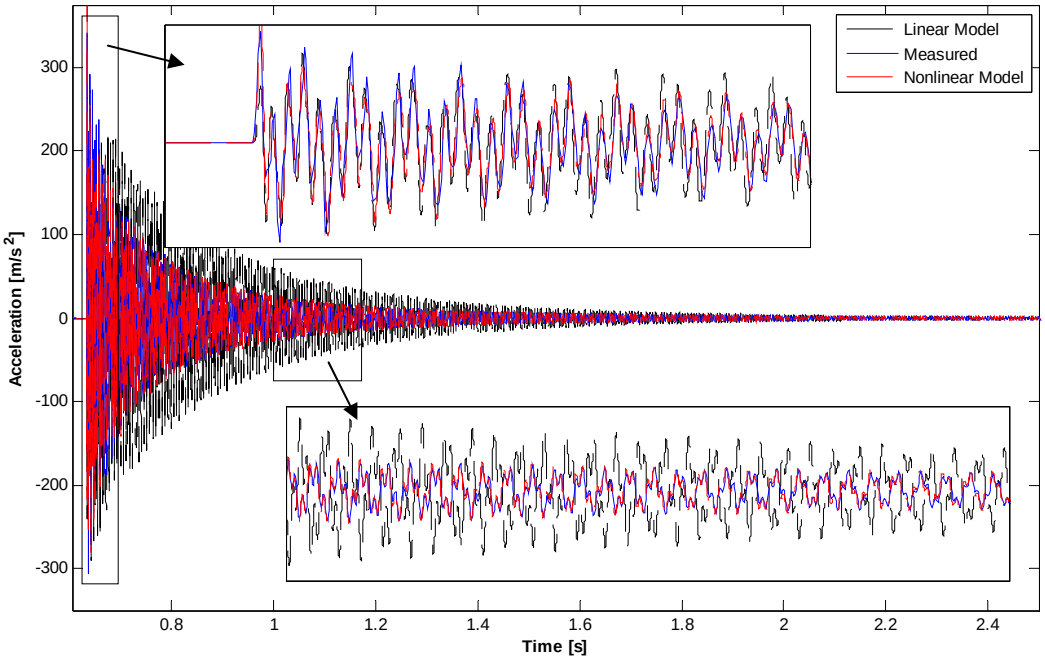

Figure 15. Drive point acceleration with the linear model

In Figure 16 one can again observe the transient response due to an impulsive load but the linear model has been removed for visual clarity. The amplitude matches fairly well in low and high amplitudes and the frequency is only off slightly later in the decay. This validates the assumption earlier that the nonlinearity in the third and fourth bending modes was sufficiently small.

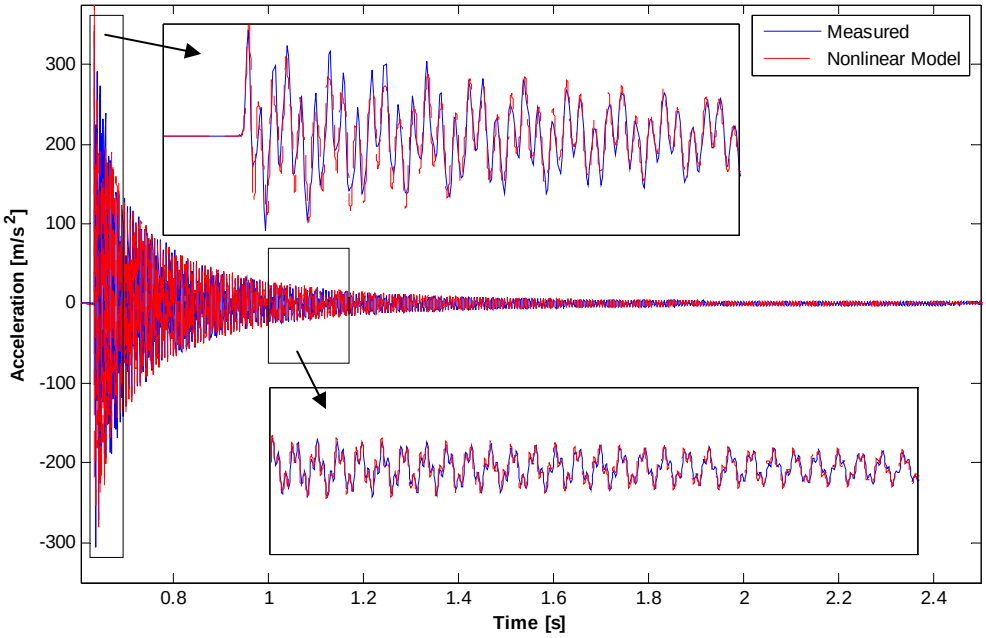

Figure 16. Drive point acceleration

Figure 17 shows the FFT of the modal acceleration for the simulated response. Enhanced views in Fig. 18 show how well the nonlinear prediction matches the true measurement. As expected based on a viewing of the time history, a linear model over predicts the amplitude by under predicting amplitude.

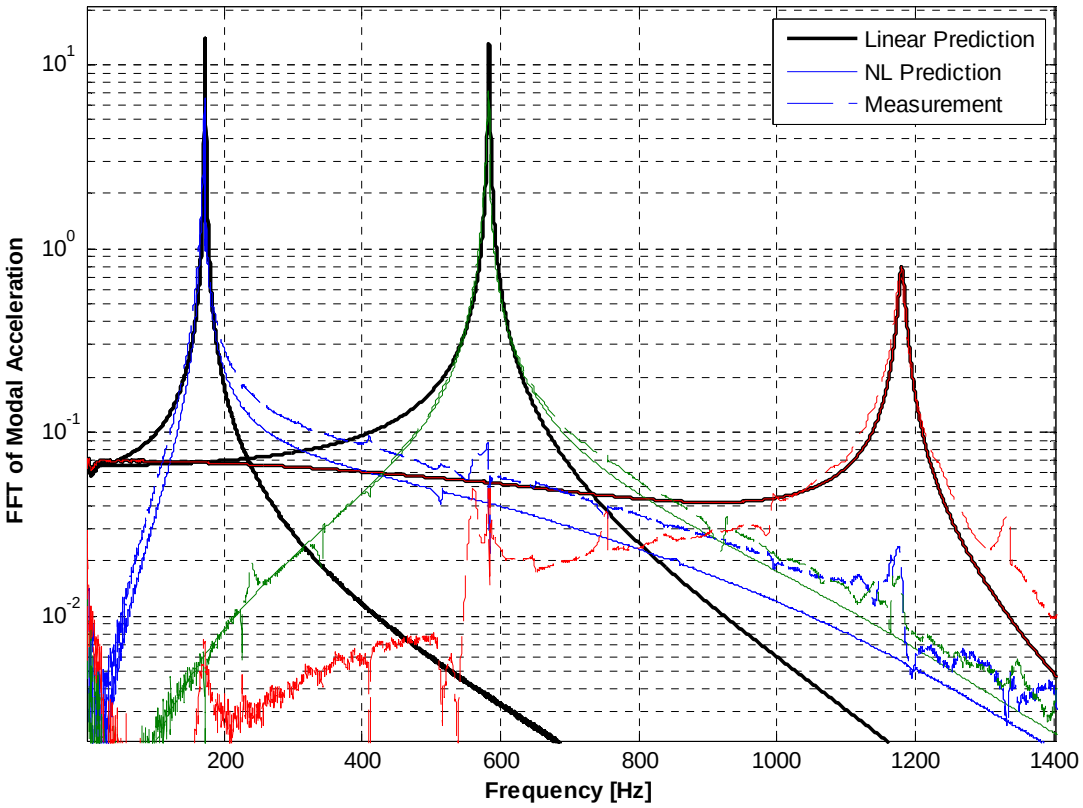

Figure 17. FFT of Modal acceleration

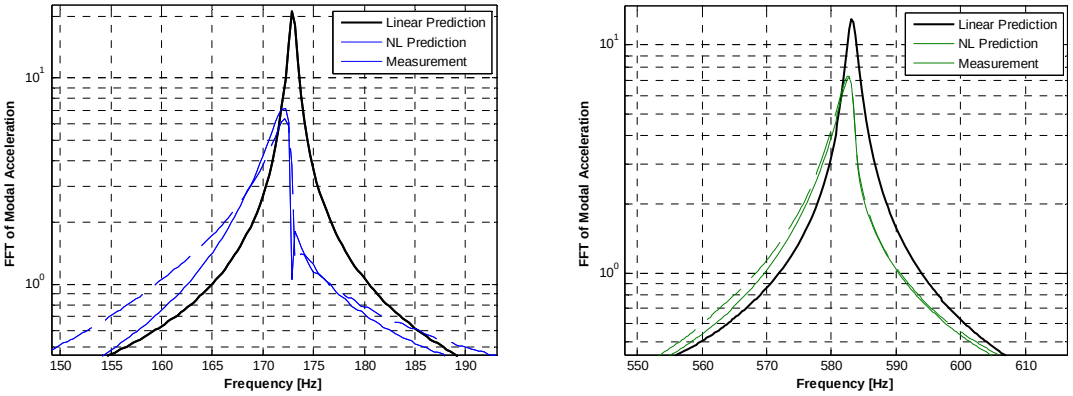

Figure 18. FFT of Modal acceleration enhanced view of elastic modes 1 (left) and 2 (right)

5. Conclusions

This work explored the applicability of a modal Iwan model for a Brake-Reuss Beam assembly. Experimental results were initially screened by examining the frequency response functions in order to determine which modes needed to be treated as nonlinear. Mirrored time history data was used with the Hilbert transform to estimate the amplitude dependent stiffness and damping behavior of each mode. Modal Iwan parameters were extracted for these nonlinear bending modes using a combination of engineering judgment, previous testing experience, and amplitude dependent stiffness and damping curves. This type of model is only accurate if the modes of the system to be reasonably spaced and remain dynamically uncoupled. Each simulated nonlinear modal model response correlated with the modally filtered measured signal well.

A nonlinear pseudo-modal model consisting of six modes was then created. This model contained two rigid modes, two nonlinear modes, and two linear modes. A simulation was conducted in which the response of this nonlinear multi-mode

model was compared to measured data in the physical domain. By just treating the first two elastic modes as nonlinear, the measured response of the system was well matched and showed great improvement over a standard linear model. By just treating the first two elastic modes as nonlinear modal models the response of the system was well represented, showing great improvement over a standard linear model.

As mentioned previously, this is one subcomponent of an assembly that we desire to study. This model is clearly superior to the standard linear model at representing this subcomponent and is therefore expected to produce a more accurate substructuring prediction. Part II [1] of this paper will explore the results of utilizing these nonlinear modal models in a component mode synthesis dynamic substructuring framework. Thus far the modes of the system have remained uncoupled. Substructuring will only succeed if the modal model is still valid even after a subcomponent is removed and added to another structure.

References

[1] D. R. Roettgen, *et al.*, "Substructuring of a nonlinear beam using modal Iwan framework, Part II: Nonlinear Modal Substructuring," presented at the International Modal Analysis Conference XXXV, Garden Grove, CA, 2017.

[2] D. J. Segalman, "An Initial Overview of Iwan Modelling for Mechanical Joints," Sandia National Laboritories, Albuquerque, New Mexico SAND2001-0811, 2001.

[3] D. J. Segalman, "A Four-Parameter Iwan Model for Lap-Type Joints," *Journal of Applied Mechanics,* vol. 72, pp. 752-760, September 2005.

[4] D. J. Segalman, "A Modal Approach to Modeling Spatially Distributed Vibration Energy Dissipation," Sandia National Laboratories, Albuquerque, New Mexico and Livermore, California SAND2010-4763, 2010.

[5] B. Deaner, Allen, M. S., Starr, M.J., Segalman, D.J., and Sumali, H., "Application of Viscous and Iwan Modal Damping Models to Experimental Measurements From Bolted Structures," *ASME Journal of Vibration and Acoustics,* vol. 137, 2015 2015.

[6] R. Lacayo, *et al.*, "A numerical study on the limitations of modal Iwan models for impulsive excitations," *Submitted to Journal of Sound and Vibration,* 2016.

[7] D. R. Roettgen and M. S. Allen, "Nonlinear characterization of a bolted, industrial structure using a modal framework," *Mechanical Systems and Signal Processing,* January 19th 2016.

[8] M. Eriten, *et al.*, "Nonlinear system identification of frictional effects in a beam with a bolted joint connection," *Mechanical Systems and Signal Processing,* vol. 39, pp. 245-264, August-September 2013 2013.

[9] M. W. Sracic, *et al.*, "Identifying the modal properties of nonlinear structures using measured free response time histories from a scanning laser Doppler vibrometer," presented at the 30th International Modal Analysis Conference Jacksonville, Florida, 2012.

[10] M. R. W. Brake, *et al.*, "Variability and Repeatability of Jointed Structures with Frictional Interfaces," presented at the International Modal Analysis Conference, Orlando, FL, 2014.

[11] E. Oberg, *Machinery's Handbook*, 29th ed.: Industrial Press, 2012.

[12] M. S. Bonney, *et al.*, "Experimental Determination of Frictional Interface Models," presented at the International Modal Analysis Conference XXXIV, Orlando, FL, 2016.

[13] S. Catalfamo, *et al.*, "Effects of Experimental Methods on the Measurements of a Nonlinear Structure," presented at the International Modal Analysis Conference XXXIV, Orlando, FL, 2016.

[14] M. S. Allen and J. H. Ginsberg, "A Global, Single-Input-Multi-Output (SIMO) Implementation of The Algorithm of Mode Isolation and Applications to Analytical and Experimental Data," *Mechanical Systems and Signal Processing,* vol. 20, pp. 1090–1111, 2006.

[15] R. D. Cook, *et al.*, *Concepts and Applications of Finite Element Analysis*, 4th Edition ed. New York: Wiley, 2002.